Reviewed Preprint
v1 • May 26, 2026
Not revised

For correspondence:
kenji.fukui@cc.nara-wu.ac.jp
takato.yano@ompu.ac.jp

Competing interests: No competing interests declared

Funding: See page 20

Reviewing editor: Axel T Brunger, Stanford University School of Medicine, Howard Hughes Medical Institute, United States

Two Glu/Asp Residues Cooperatively Mediate an Early Step of ATP Hydrolysis in GHKL ATPases MutL and GyrB

Kenji Fukui[1,2], **Ayaka Shibuya**[1], **Takeshi Murakawa**[3], **Takato Yano**[1]

[1]Department of Biochemistry, Faculty of Medicine, Osaka Medical and Pharmaceutical University, Takatsuki, Japan • [2]Department of Food Science and Nutrition, Faculty of Human Life and Environment, Nara Women's University, Nara, Japan • [3]Department of Chemistry, Faculty of Medicine, Osaka Medical and Pharmaceutical University, Takatsuki, Japan

eLife Assessment

In this **solid** work, Fukui et al. re-examined the ATP hydrolysis mechanism in GHKL ATPases, revealing a cooperative role for two conserved acidic residues rather than a single one. This **useful** study used a range of biochemical and structural techniques on various mutants from different members of the GHKL ATPase family to test and validate their proposed mechanism. An updated and extended mechanistic model of ATP hydrolysis by this class of enzymes is proposed.

https://doi.org/10.7554/eLife.111443.1.sa2

Abstract

GHKL ATPases share a unique Bergerat ATP-binding fold and regulate diverse biological processes through ATP-dependent conformational changes. An early step of ATP hydrolysis in this family has been attributed to a single highly conserved glutamate residue proposed to function as the general base. However, mutations of this residue impair both the ATPase activity and ATP binding, complicating interpretation of its catalytic role. Re-examination of the high-resolution crystal structures revealed a second conserved acidic residue positioned within a hydrogen-bonding distance from the nucleophilic water molecule. Using *Aquifex aeolicus* MutL and GyrB as model enzymes, we combined systematic mutagenesis, ATPase and ATP-binding assays, and X-ray crystallography to dissect the roles of these residues. We show that alignment of the nucleophilic water can be maintained as long as the conserved glutamate retains hydrogen-bonding capability, whereas efficient ATP hydrolysis requires proton-accepting capacity at least one of the two acidic residues. These results indicate that the conserved glutamate primarily governs positioning of the nucleophilic water, while activation of this water for catalysis is achieved through cooperative general base function of the two acidic residues. Extending this framework to human MutL homologs, PMS2 and MLH1, we showed that clinically reported variants of uncertain significance in these DNA mismatch repair proteins substantially reduced the ATPase activity, indicating functional impairment. Together, our findings refine the catalytic mechanism of GHKL ATPases and provide a structural and functional framework for interpreting disease-associated variants in GHKL ATPases. Phylogenetic and ancestral state analysis further indicated that the second acidic residue was likely to be present in the common ancestor of major GHKL ATPase lineages but was later modified in a branch including Hsp90, suggesting evolutionary remodeling of the catalytic mechanism in the branch.

Introduction

The GHKL ATPase family comprises a wide range of proteins involved in diverse cellular processes, including DNA replication, DNA repair, protein homeostasis, chromatin regulation, and signal transduction [1]. The GHKL ATPase family includes the following representative members: DNA gyrase B (GyrB), the ATPase subunit of type II topoisomerase that introduces negative supercoils into DNA [2,3]; the molecular chaperone Hsp90, which regulates the folding and stability of numerous client proteins [4]; histidine kinases of two-component regulatory systems, which function in environmental sensing and signal transduction [5]; the DNA mismatch repair protein MutL, which maintains genome stability by correcting replication errors [6,7]; and MORC family proteins, which contribute to chromatin organization and epigenetic regulation [8,9]. Despite their functional diversity, these proteins share a conserved Bergerat ATP-binding motif and are thought to employ a common mechanism for ATP binding and hydrolysis [1,10–13].

For GHKL ATPases, ATPase activity is essential for protein function. In many cases, ATP binding and hydrolysis drive large-scale conformational changes that are coupled to biological activity. The ATP-bound and ADP-bound states often correspond to distinct oligomeric or domain arrangements, and cycling between these states enables GHKL ATPases to act as molecular switches or motors that coordinate complex cellular processes [14–16]. A representative example of such functional coupling is provided by MutL, a key component of the DNA mismatch repair pathway [17–19]. MutL consists of an N-terminal ATPase domain and a C-terminal nuclease domain, and ATP binding induces dimerization of the N-terminal domains, leading to rearrangement of the overall architecture and engagement of downstream repair factors [14,20–22]. Subsequent ATP hydrolysis, stimulated by interacting proteins and DNA substrates, induces further conformational changes that activate its nuclease function and enable strand incision during mismatch repair [7,23–25]. Thus, in MutL, the ATP binding and hydrolysis cycle directly controls large-scale structural transitions that are essential for its biological activity. A detailed understanding of the ATP hydrolysis mechanism is therefore crucial not only for elucidating the molecular basis of fundamental biological phenomena but also for clarifying disease mechanisms associated with dysfunction of GHKL ATPases.

In human, impaired function of MutL proteins compromises the DNA mismatch repair pathway, leading to reduced fidelity of DNA replication. Such defects are a major cause of Lynch syndrome, one of the most common hereditary cancer predisposition syndromes [26–30]. Cancers associated with Lynch syndrome exhibit high responsiveness to immune checkpoint inhibitors [31,32], and genetic testing of MutL genes is recommended for diagnosis. However, clinical interpretation is often hampered by the presence of variants of uncertain significance. This limitation largely reflects the insufficient understanding of MutL function at the amino acid level. Variants of uncertain significance have also been identified in the ATPase active site of human MutL homologs, highlighting the importance of elucidating the ATP hydrolysis mechanism of MutL for establishing a molecular basis for genetic diagnosis of Lynch syndrome.

Among GHKL ATPases, GyrB, MutL, and MORC are thought to share particularly similar ATPase mechanisms [11]. Within the Bergerat ATP-binding motif, a highly conserved glutamate residue, Glu29 in *Aquifex aeolicus* MutL (aqMutL), has been proposed to function as a general base that activates the nucleophilic water molecule for ATP hydrolysis [33,34]. This proposal is based on observations that substitution of alanine or lysine for this glutamate abolishes the ATPase activity. In addition, a conserved lysine residue, Lys79, in aqMutL, has been suggested to act as a general acid, donating a proton to the reaction intermediate and thereby facilitating cleavage of the γ-phosphate [11]. Other conserved basic residues have also been proposed to contribute as Lewis acids that stabilize negatively-charged reaction intermediates [11,34]. Collectively, these residues have been proposed to form the core catalytic machinery of GHKL ATPases.

Previously, we determined high-resolution crystal structures of the ATPase domain of aqMutL in complex with ATP analogs, in which a water molecule presumed to be the nucleophile for ATP hydrolysis was clearly observed at a hydrogen-bonding distance to the conserved glutamate Glu29 [35]. Upon careful re-examination of these structures, we noticed that this same water molecule is

also positioned within a hydrogen-bonding distance to a second conserved acidic residue, Glu32 (Fig. 1A). Thus, the nucleophilic water is not exclusively coordinated by Glu29, but simultaneously interacts with two acidic residues.

Although earlier biochemical studies, including those from our group, demonstrated that replacement of Glu29 with alanine abolishes the ATPase activity, such mutations also severely impair ATP binding [11,33], complicating interpretation of the specific catalytic role of this residue. In this context, the potential contribution of Glu32 to ATP hydrolysis might have been overlooked. Supporting this notion, the residue corresponding to Glu32 is conserved not only in MutL but also in other GHKL ATPases, including GyrB and MORC proteins (Fig. 1B). Furthermore, replacements of the corresponding Glu residue with Lys in *Escherichia coli* MutL and in human MutL homolog 1 (MLH1) have been reported to abolish DNA mismatch repair activity in cell-based or nuclear extract-based assays [36,37].

In this study, we investigated the functional role of Glu32 in the ATP hydrolysis mechanism of MutL and GyrB using a combination of enzymatic and X-ray crystallographic analyses. Our results provide new insights into the catalytic mechanism of GHKL ATPases and refine the current model of ATP hydrolysis for this protein family. By clarifying the molecular basis of ATP hydrolysis in GHKL ATPases, this work also provides a mechanistic framework for interpreting the functional consequences of some clinically observed variants, thereby contributing to the foundation for assessing the impact of variants of uncertain significance.

Results and Discussion

Mutational analysis of Glu29 and Glu32 in the ATPase domain of aqMutL

To examine the contribution of Glu32 to the ATPase activity of the aqMutL NTD and to directly compare its role with that of Glu29, we introduced a series of substitutions at both positions. To exclude the possibility that the observed effects on the ATPase activity arose from global structural perturbations, circular dichroism (CD) spectra were measured for all mutant forms (Fig. 2A). Among these, only the E32G mutant form exhibited a marked decrease in ellipticity, suggesting that this substitution disrupts the secondary structure of the protein. In contrast, all other mutant forms displayed CD spectra indistinguishable from that of the wildtype form, indicating that these substitutions do not substantially perturb the overall structure of the aqMutL NTD.

We first analyzed the effects of mutations at Glu29 on the ATPase activity of the aqMutL NTD. The mutation to Gln would selectively impair the proton association/dissociation capability of the Glu side chain while preserving its size and hydrogen-bonding potential. Moreover, because mutations to Val, Lys, and Gly at this position have been reported as variants of uncertain significance in human MutL, these mutations were also analyzed. Consistent with previous reports, all Glu29 mutant forms exhibited severe reduction in the ATPase activity (Fig. 2B and C, and Table 1). In particular, the E29A, E29V, E29K, and E29G mutant forms showed activities below the detection limit, indicating that Glu29 plays a central role in ATP hydrolysis. However, as described above, previous studies also demonstrated that mutations at Glu29 impair ATP binding [11,33,34], indicating that the loss of the ATPase activity of these mutant forms cannot be unambiguously attributed to disruption of a catalytic base function.

To further dissect the role of Glu29, we focused on the E29Q mutant form. Using equilibrium dialysis, we confirmed that the E29Q mutant form binds ATP with an affinity comparable to that of the wildtype protein (Supplementary Fig. S1A). Because this substitution does not impair ATP binding, it should enable a more direct assessment of the proposed role of Glu29 as a general base in ATP hydrolysis. The E29Q mutant form retained measurable ATPase activity, although its k_{cat} value was approximately tenfold smaller than that of the wildtype enzyme (Fig. 2B and C, and Table 1). The persistence of substantial catalytic activity in the absence of the carboxylate group at the position 29 suggests that a residue other than Glu29 can participate in proton abstraction from the nucleophilic water during ATP hydrolysis.

Figure 1. Structural position and conservation of two acidic residues in the GHKL ATPase family.

(A) Crystal structure of the aqMutL N-terminal domain (NTD) in complex with the non-hydrolyzable ATP analog AMPPCP. The boxed region indicates the ATP-binding site and is shown enlarged on the right. AMPPCP and the side chains of Glu29 and Glu32 are shown as stick models. Oxygen atoms are shown in red, nitrogen atoms in blue, and phosphorus atoms in orange. The magnesium ion and the water molecule putatively acting as the nucleophile are depicted as green and red spheres, respectively. Hydrogen bonds are indicated by dashed lines, with distances shown. The blue mesh represents an omit F_o–F_c electron density map contoured at 3σ for AMPPNP, the magnesium ion, and the water molecule. (B) Sequence alignment of representative GHKL ATPases. The Bergerat ATP-binding fold is underlined, and the conserved acidic residues corresponding to aqMutL Glu29 and Glu32 are marked with asterisks. Amino acid sequence alignment was performed by CLUSTAL W program [57] and visualized by ESPript3 [58].

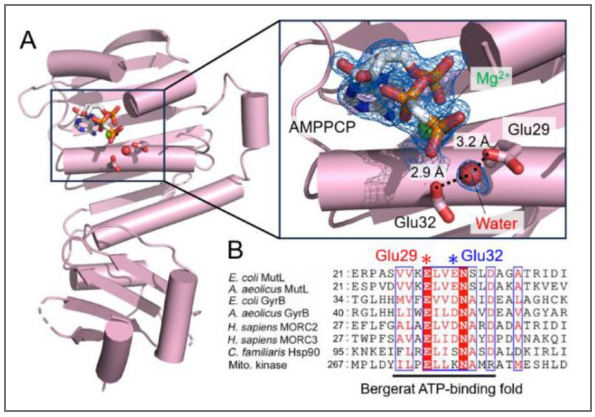

Figure 2. Effects of mutations on the overall structure and the ATPase activity of the aqMutL NTD.

(A) Far-UV CD spectra of the wildtype and mutant forms of the aqMutL NTD were collected and averaged over 10 consecutive scans. (B, C) ATPase activity of the aqMutL NTD was measured under steady-state conditions using a colorimetric assay that detects the release of inorganic phosphate. Apparent rate constants (k_{app}) were calculated from the measured phosphate concentrations and plotted as a function of ATP concentration. Kinetic parameters were determined by fitting Michaelis–Menten equation to the data. Each data point represents the mean of three independent experiments, with error bars indicating standard deviation. Theoretical curves calculated from the fitted kinetic parameters are overlaid. Data for 0–1 mM substrate concentrations are shown to compare the wildtype from with mutant forms (B). Activities for higher substrate concentrations were measured for some of the mutant forms (C).

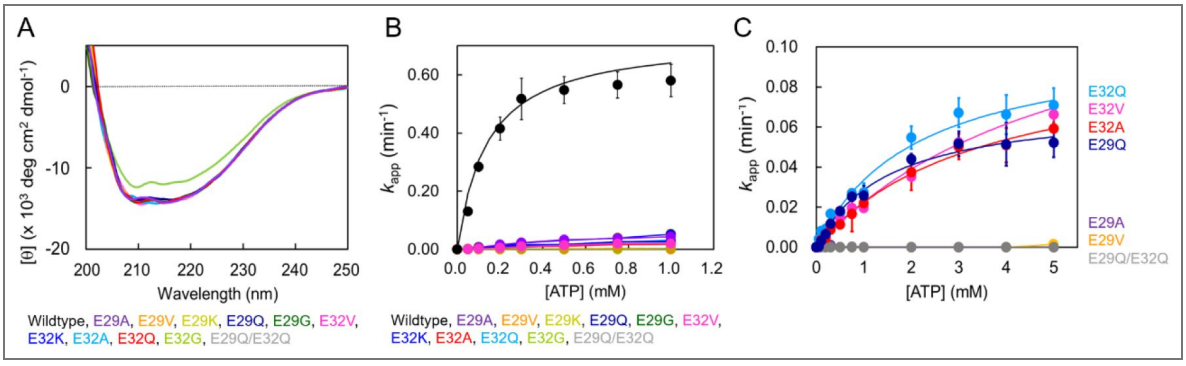

Proteins	k_{cat} (min^{-1}) [1]	K_m (mM) [1]	k_{cat}/K_m (M^{-1} s^{-1})
aqMutL WT	0.65 ± 0.10	0.14 ± 0.026	77
E29A	N.D.[2]	N.D.[2]	N.D.[2]
E29V	N.D.[2]	N.D.[2]	N.D.[2]
E29K	N.D.[2]	N.D.[2]	N.D.[2]
E29Q	0.069 ± 0.010	1.5 ± 0.20	0.77
E29G	N.D.[2]	N.D.[2]	N.D.[2]
E32A	0.10 ± 0.022	2.1 ± 0.39	0.79
E32V	0.15 ± 0.057	5.5 ± 1.3	0.45
E32K	N.D.[2]	N.D.[2]	N.D.[2]
E32Q	0.10 ± 0.018	3.5 ± 0.46	0.48
E32G	N.D.[2]	N.D.[2]	N.D.[2]
E29Q/E32Q	N.D.[2]	N.D.[2]	N.D.[2]
aqGyrB NTD WT	2.4 ± 0.19	0.35 ± 0.066	110
E48A	N.D.[2]	N.D.[2]	N.D.[2]
E48Q	0.78 ± 0.16	0.75 ± 0.34	13
D51A	0.39 ± 0.024	0.21 ± 0.038	31
D51N	1.2 ± 0.18	0.28 ± 0.059	137
E48Q/D51N	N.D.[2]	N.D.[2]	N.D.[2]
human PMS2 NTD WT	0.62 ± 0.049	0.51 ± 0.14	20
E44Q	0.13 ± 0.011	0.22 ± 0.079	9.8
E44V	0.085 ± 0.069	0.67 ± 0.14	2.1
human MLH1 NTD WT	0.12 ± 0.046	0.66 ± 0.064	3.0
E37K	N.D.[2]	N.D.[2]	N.D.[2]

[1]The standard Michaelis-Menten equation was fitted to the data to determine the k_{cat} and K_m values.
[2]N.D. means that the activity was not detected.

Table 1. Kinetic parameters for the ATPase activity of the aqMutL NTDs, aqGyrB NTDs, ProS2-tagged human PMS2 NTDs, and histidine-tagged human MLH1 NTDs.

We next examined the effects of mutations at Glu32. Mutations of Glu32 resulted in reduced ATPase activity relative to the wildtype form, supporting a role for this residue in catalysis. However, with the exception of the E32K and the structurally perturbed E32G mutant forms, all Glu32 mutant forms retained detectable ATPase activity (Fig. 2B and C, and Table 1), indicating that loss of Glu32 alone is insufficient to abolish ATP hydrolysis. Simultaneous substitutions of glutamine for the two residues in the E29Q/E32Q double mutant form led to a complete loss of the ATPase activity. Taken together, these results indicate that Glu29 and Glu32 do not exert equivalent functions but act cooperatively. The presence of at least one carboxylate group at either position, 29 or 32, appears to be required for ATP hydrolysis.

Conserved roles of two acidic residues of aqGyrB in ATP hydrolysis

To examine whether the cooperative roles of Glu29 and Glu32 observed in aqMutL are conserved among other GHKL ATPases, we next analyzed the NTD of *A. aeolicus* GyrB (aqGyrB). A glutamate residue corresponding to aqMutL Glu29 is also conserved in bacterial GyrB and has been proposed to function as a general base in ATP hydrolysis [38]. Although crystal structure of the *E. coli* GyrB NTD has been reported [39], the position of the putative nucleophilic water has not been clearly defined. Therefore, we selected the GyrB NTD from the hyperthermophilic bacterium *A. aeolicus* as a model system, anticipating that it would allow high-resolution structural analysis and clearer visualization of a catalytic water molecule.

First, we determined the crystal structure of this protein in complex with AMPPNP at 1.65 Å resolution (Table 2 and Fig. 3). The overall structure was highly similar to that of the *E. coli* GyrB NTD, with a Cα root mean square deviation of 1.42 Å. As observed for the *E. coli* GyrB NTD, AMPPNP was accommodated by the Bergerat ATP-binding fold, and AMPPNP binding seemed to induce conformational changes that promoted dimer formation through the newly formed interface. Glu48 and Asp51 of aqGyrB correspond to Glu29 and Glu32 of aqMutL, respectively. In the crystal structure, these residues were found to tightly coordinate a water molecule that is likely to act as the nucleophilic water during ATP hydrolysis (Fig. 3). Based on these structural observations, we introduced Ala or Gln/Asn substitutions for Glu48 and Asp51. The CD spectra of the mutant forms were nearly identical to that of the wildtype form (Fig. 4A), suggesting that these substitutions did not disrupt the overall structure of the aqGyrB NTD.

Equilibrium dialysis showed that the E48A mutant form failed to bind ATP, whereas the E48Q mutant form displayed ATP-binding affinity comparable to that of the wildtype protein (Supplementary Fig. S1B). The E48Q mutation therefore allowed us to evaluate the catalytic contribution of Glu48 independently of ATP binding. ATPase activity assays showed that the E48A mutant form completely lacked the activity, while the E48Q mutant form retained approximately one quarter of the wildtype activity (Fig. 4B and Table 1). The persistence of substantial catalytic activity in the E48Q mutant form suggests that another residue partially compensates for the loss of the Glu48 carboxylate in the proton abstraction. Mutations of Asp51 also impaired ATP hydrolysis, with the D51A and D51N mutant forms retaining ~25% and ~50% of the wildtype activity, respectively (Fig. 4B and Table 1). Notably, the E48Q/D51N double mutant form exhibited no detectable ATPase activity, resembling the effect of the corresponding double mutation in the aqMutL NTD. Taken together, these results indicate that both Glu48 and Asp51 contribute to the catalytic mechanism of ATP hydrolysis in aqGyrB and that at least one of these residues must retain a carboxylate group with the proton-accepting capability to sustain the enzymatic activity.

Crystal structures of aqGyrB mutant forms and the role of Glu48 in ATP binding

Figure 3. **Structure of the AMPPNP-bound dimer of the wildtype aqGyrB NTD.**

The boxed region highlights the ATP-binding site and is enlarged in the left panel. The same region is further enlarged and rotated 60° to provide an alternative view of the active site geometry. AMPPNP and the side chains of Glu48 and Asp51 are shown as stick models. Oxygen atoms are shown in red, nitrogen atoms in blue, and phosphorus atoms in orange. The magnesium ion and the water molecule presumed to act as the nucleophile are depicted as green and red spheres, respectively. Hydrogen bonds are indicated by dashed lines, with distances shown. The blue mesh represents an omit F_o–F_c electron density map contoured at 3σ for AMPPNP, the magnesium ion, and the water molecule.

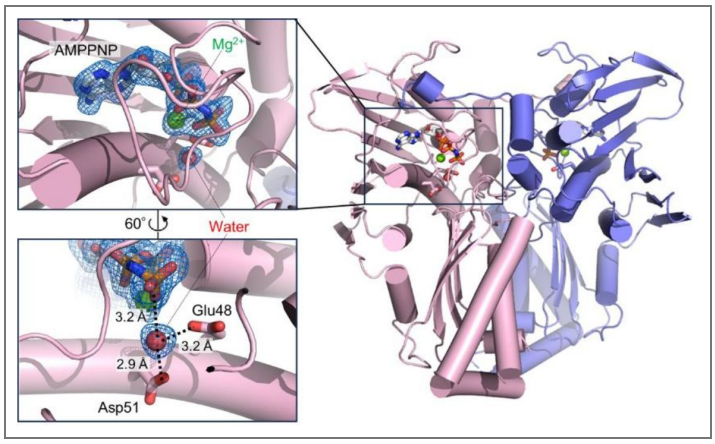

Figure 4. **Effects of mutations on the overall structure and the ATPase activity of the aqGyrB NTD.**

(A) Far-UV CD spectra of the wildtype and mutant forms of the aqGyrB NTD were recorded and averaged over 10 accumulations. (B) ATPase activity of the aqGyrB NTD was measured under steady-state conditions as described in Fig. 2. The k_{app} values were plotted as a function of ATP concentration. Michaelis–Menten equation was fitted to the data. Data points represent the mean ± standard deviations from three independent experiments.

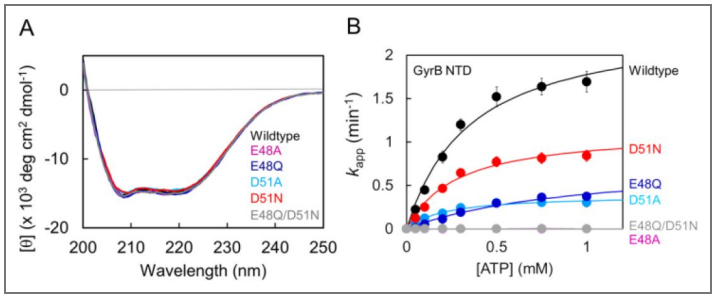

In order to relate the ATPase activity profiles of the mutant forms to their structural features, we determined X-ray crystal structures of selected mutant forms using the aqGyrB NTD as a model system, which allows relatively high-resolution structural analyses. The AMPPNP-bound structures of the E48A, E48Q, D51A, and D51N mutant forms were determined at resolutions of 2.66, 1.70, 1.63, and 2.05 Å, respectively (Table 2).

Since the conserved general base Glu (i.e. Glu48 of aqGyrB) does not directly interact with ATP, it has been unclear why mutations at the Glu residue abolish the ATP-binding ability of GHKL ATPases. To clarify this, we compared the crystal structures of the wildtype and mutant forms of the aqGyrB NTD (Fig. 5). In GHKL ATPases, ATP binding is tightly coupled to conformational rearrangements, including formation of an ATP lid (Fig. 5A), which acts to secure the bound nucleotide by enclosing it within the active site [3,21]. Structural analysis of the wildtype aqGyrB NTD revealed that the side chain of Glu48 forms a hydrogen bond with Gln340, thereby stabilizing a loop containing Gln340 in a conformation capable of ATP binding (Fig. 5B). In this arrangement, Gln340 in turn forms a hydrogen bond with His122, a residue located within the ATP lid, while Lys342 in the same loop is positioned to interact with the γ-phosphate of ATP. These coordinated interactions appear to promote the ATP-induced conformational transition required for stable nucleotide binding.

In contrast, structural analysis of the E48A mutant form demonstrated that disruption of the interaction with Gln340 abolishes this network of hydrogen bonds, preventing the associated conformational rearrangements and thereby impairing ATP binding (Fig. 5C). These findings indicate that the interaction network emanating from Glu48 is indispensable for the conformational changes associated with the ATP lid formation. Interestingly, in the E48Q mutant form, the hydrogen bond with Gln340 is preserved, allowing the conformational transition to occur and enabling ATP binding (Fig. 5D). Consistently, in the D51A and D51N mutant forms, the interaction mediated by Glu48 remains intact, and the structural rearrangements required for ATP binding are maintained (Fig. 5E and F).

These structural observations extend previous models of GyrB ATPase function by linking the conserved catalytic glutamate to ATP lid stabilization and nucleotide-dependent conformational rearrangement. The E48A aqGyrB NTD structure, in particular, provides direct structural evidence that disruption of this Glu-centered interaction network is sufficient to prevent ATP-induced active-site assembly. This hydrogen-bonding network emanating from the general base Glu is conserved in GyrBs from other organisms [39,40] (Supplementary Fig. S2), while it is not observed in other GHKL ATPases, including MutL [22,34,35,41] and MORC family proteins [9,42,43]. Therefore, the loss of ATP-binding ability observed upon the mutation of Glu29 to Ala in MutL [11] is likely to be explained by a different mechanism. This difference highlights mechanistic diversity within the GHKL ATPase family, despite conservation of the two catalytic acidic residues.

Nucleophilic water molecule in the active site of mutant forms of the aqGyrB NTD

Having established the structural basis for the altered ATP-binding properties of the mutant forms, we next analyzed how these substitutions influence the positioning of the nucleophilic water molecule. Structural comparisons of the catalytic sites of the four mutant forms are shown in Fig. 6. In the E48A mutant form (Fig. 6A), the nucleophilic water molecule was not observed in the catalytic site. In contrast, in the E48Q mutant form, the nucleophilic water molecule was positioned at essentially the same location as in the wildtype form, coordinated by Gln48 and Asp51, and bound AMPPNP was observed (Fig. 6B). This structural arrangement is consistent with the biochemical data described above, in which the E48Q mutant form retained substantial ATP-binding and ATPase activities.

Unlike the E48A mutant form, the D51A mutant form bound AMPPNP (Fig. 6C), and the nucleophilic water molecule was coordinated only by Glu48. This asymmetric coordination suggests that Glu48 plays a dominant role in positioning the nucleophilic water molecule. In the D51N mutant form (Fig. 6D), which lacks the proton-transfer capability of Asp51 while retaining

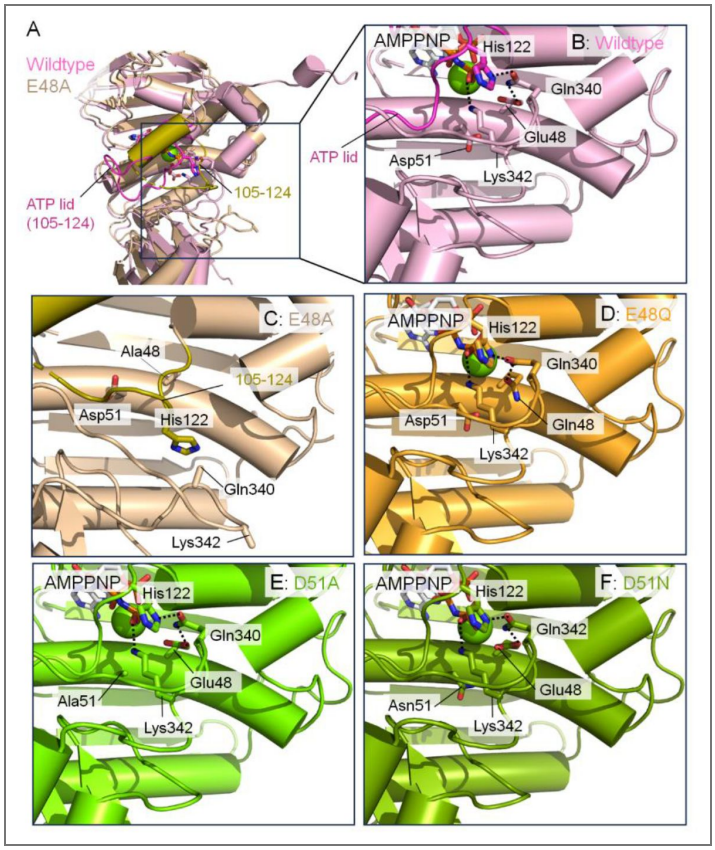

Figure 5. Structural basis for the loss and preservation of ATP binding in aqGyrB NTD mutant forms.

The wildtype and all mutant forms were crystallized in the presence of AMPPNP; however, the E48A mutant form did not bind AMPPNP, whereas the E48Q, D51A, and D51N mutant forms were observed in complex with AMPPNP. (A) Overall structures of the wildtype and E48A mutant aqGyrB NTD monomers. The ATPase active site is indicated by a boxed region. The ATP-lid (residues 105–124) in the wildtype form and the corresponding region in the E48A mutant form are shown in magenta and olive, respectively. (B–F) Enlarged views of the ATPase active site in the wildtype (B), E48A (C), E48Q (D), D51A (E), and D51N (F) forms. Side chains of the residues implicated in the ATP-induced conformational changes (e.g. His122, Gln340, and Lys342), as well as residues 48 and 51, are shown as stick models. AMPPNP is depicted as sticks, and the Mg^{2+} ion is shown as a green sphere. Hydrogen bonds and ionic interactions are indicated by dashed lines.

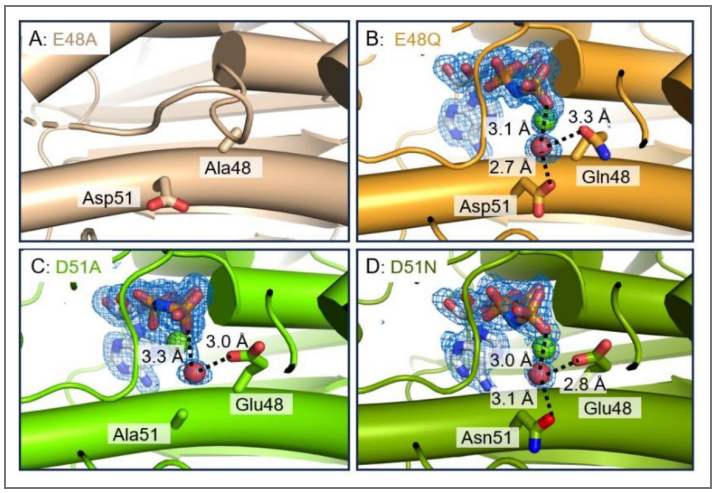

Figure 6. Structures surrounding the conserved acidic residues: (A) E48A, (B) E48Q, (C) D51A, and (D) D51N mutant forms of the aqGyrB NTD.

AMPPNP and the side chains at the positions 48 and 51 are shown as stick models. Oxygen atoms are shown in red, nitrogen atoms in blue, and phosphorus atoms in orange. The magnesium ion is shown as a green sphere, and the water molecule proposed to act as the nucleophilic water is shown as a red sphere. Blue mesh represents F_o–F_c omit electron density maps contoured at 3σ, calculated after omission of AMPPNP, the magnesium ion, and the nucleophilic water molecule. Hydrogen bonds are indicated by dashed lines, with the corresponding distances shown.

its hydrogen-bonding capacity, the nucleophilic water was coordinated by both Glu48 and Asn51. These structural features are consistent with the relative ATPase activities observed for the mutant forms of these two acidic residues (Fig. 4B).

Taken together, these results indicate that Glu48 and Asp51 make distinct yet cooperative contributions to ATP hydrolysis. Glu48 appears to play a dominant role in aligning the nucleophilic water molecule and activating this water molecule through proton abstraction as a general base. In contrast, Asp51 seems to contribute less to the precise positioning of the nucleophilic water but participates cooperatively with Glu48 in the proton abstraction, thereby supporting efficient ATP hydrolysis. Notably, an acidic residue corresponding to Asp51 of aqGyrB is conserved among several GHKL ATPases, including MutL, GyrB, and MORC family proteins (Fig. 1B), suggesting that the two-acidic-residue mechanism proposed here may be shared among these subgroups. The second acidic residue is not conserved in other members of the GHKL family, such as Hsp90 and mitochondrial histidine kinases (Fig. 1B), where a single acidic residue is thought to fully function as the general base responsible for water activation. A similar divergence appears to apply to the previously-reported general acid Lys residue [11], further supporting the notion that GHKL ATPases can be divided into at least two mechanistically distinct subclasses. This mechanistic bifurcation provides insights into the molecular evolution of the GHKL ATPase family.

Functional and clinical implications of the second acidic residue in human MutL homologs

Our analyses of the aqMutL NTD and aqGyrB NTD indicate that, in addition to the Glu residue traditionally considered to function as the general base, an additional conserved acidic residue (Glu or Asp) also participates in the general base catalysis. In human MutL homologs, this residue corresponds to Glu44 in Postmeiotic Segregation Increased 2 (PMS2) and Glu37 in MLH1. Notably, variants of uncertain clinical significance, including E44V (ClinVar variation ID: 232732), E44G (230139), and E44Q (186069) in PMS2, as well as E37G (230139) and E37K (89640) in MLH1, have been reported at these positions.

To examine whether these residues similarly contribute to the ATPase activity in human MutL homologs, we introduced the corresponding mutations into the NTDs of human PMS2 and MLH1 and measured their ATPase activities. The recombinant E44G human PMS2 NTD and E37G human MLH1 NTD could not be expressed successfully, which is consistent with our finding that the corresponding mutation in the aqMutL NTD disrupted the structural integrity of the protein (Fig. 2A). Both the E44V and E44Q mutant forms of the PMS2 NTD exhibited a marked reduction in the ATPase activity, retaining approximately one-sixth of the wildtype activity (Fig. 7A and Table 1). In contrast, the E37K mutation in the MLH1 NTD completely abolished the ATPase activity under our assay conditions (Fig. 7B and Table 1).

These results are in good agreement with our observations for the aqMutL NTD and aqGyrB NTD, further supporting the notion that this second acidic residue plays a conserved and functionally significant role in ATP hydrolysis across the GHKL ATPase family. Previous studies demonstrated that even a several-fold reduction in the MutL ATPase activity could severely compromise mismatch repair efficiency *in vivo* [11]. In this context, the substantial reduction in the ATPase activity caused by the E44V and E44Q mutations in the PMS2 NTD is likely to impair mismatch repair in human cells. Therefore, these variants might contribute to the development of Lynch syndrome by weakening the ATPase-driven regulatory functions of MutL. Nevertheless, whether these variants indeed compromise mismatch repair activity *in vivo* remains to be directly tested. Functional validation using cell-based or nuclear extract-based mismatch repair assays, such as the 6-thioguanine sensitivity assay [44] or CIMRA assay [36], will be required to establish a definitive link between the reduced ATPase activity and mismatch repair deficiency in human cells.

Figure 7. ATPase activities of human MutL homolog NTDs.

(A) ATPase activity of mutant forms of the human PMS2 NTD. (B) ATPase activity of a mutant form of the human MLH1 NTD. ATPase activities were measured using the same procedures as described for Fig. 2 and Fig. 4. Apparent rate constants (k_{app}) were plotted as a function of substrate concentration. Data points represent the mean values from three independent measurements, with error bars indicating standard deviations. Solid lines represent the theoretical Michaelis-Menten curves.

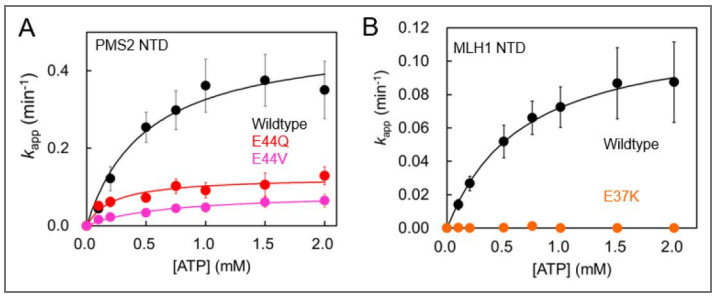

Figure 8. Maximum-likelihood phylogeny of the ATPase domain of representative GHKL family members.

The state of the amino acid residue at the position corresponding to aqMutL Glu32 or aqGyrB Asp51 is indicated by colored bars (red, acidic residue; blue, non-acidic residue). The phylogenetic tree was visualized and annotated using the Interactive Tree of Life (iTOL) web server [56]. The tree is displayed in a rectangular layout for clarity and should be interpreted as unrooted. Ancestral state reconstruction was performed on the fixed topology, and posterior probabilities are shown for selected internal nodes. The internal node uniting the MutL/GyrB/MORC/Hsp90 clades strongly supports an acidic residue with the posterior probability (PP) of 0.983, whereas the Hsp90 stem ancestor is strongly supported to encode serine at this position with the posterior probability of 1.000. Species abbreviations used in the phylogenetic tree are as follows: Ce, *Caenorhabditis elegans*; Sc, *Saccharomyces cerevisiae*; Dr, *Danio rerio*; Hs, *Homo sapiens*; Aa, *Aquifex aeolicus*; Hp, *Helicobacter pylori*; Tt, *Thermus thermophilus*; Ec, *Escherichia coli*; Mt, *Mycobacterium tuberculosis*; Bs, *Bacillus subtilis*; Sm, *Streptococcus mutans*; Dm, *Drosophila melanogaster*; Clf, *Canis lupus familiaris*; Mm, *Mus musculus*; Hc, *Hemicordylus capensis*; Pv, *Patella vulgata*; Tf, *Tachysurus fulvidraco*; Lk, *Lepidochelys kempii*; Cc, *Castor canadensis*; Dn, *Dasypus novemcinctus*.

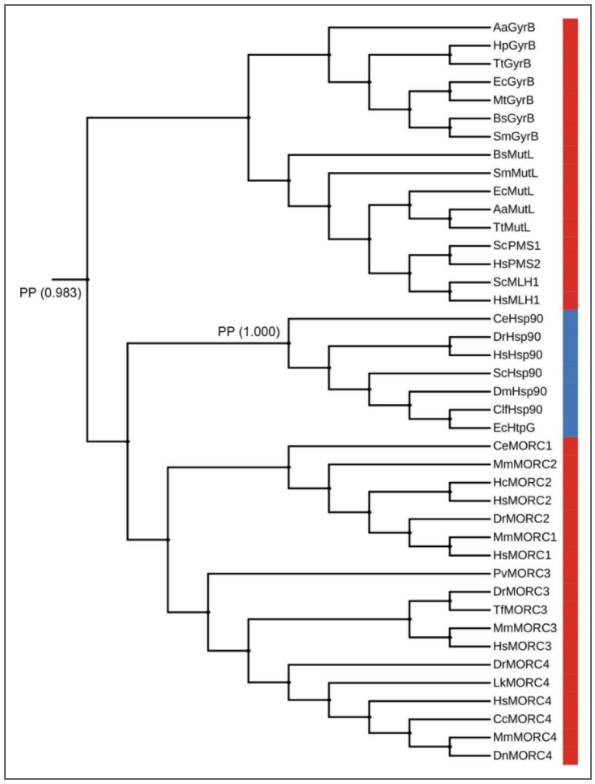

Phylogenetic analysis of GHKL ATPases

The newly-identified functionally-important acidic residue is not uniformly conserved across the GHKL superfamily. We therefore used this position as an evolutionary marker to investigate patterns of molecular divergence within the GHKL ATPase domain. In histidine kinases, even the canonical catalytic glutamate is typically replaced, and the ATPase-associated catalytic machinery is not maintained [1,45,46]. Therefore, phylogenetic reconstruction was restricted to other GHKL ATPase family members MutL, GyrB, MORC, and Hsp90.

Phylogenetic analysis based on the trimmed ATPase-domain alignment recovered these major GHKL ATPase lineages (MutL, GyrB, MORC, and Hsp90) as a well-supported cluster, indicating relatively close evolutionary relationships among these groups, which is consistent with a previous study [1]. Ancestral state reconstruction performed on the maximum-likelihood phylogeny strongly supports the presence of an acidic residue at the position corresponding to aqMutL Glu32 or aqGyrB Asp51 in the internal node uniting the MutL, GyrB, MORC, and Hsp90 clades with a posterior probability of 0.983. In contrast, the ancestral node of the Hsp90 clade is strongly supported to encode serine at this position with a posterior probability of 1.000. Because no external outgroup was specified, the global polarity of amino acid residue changes across the entire phylogeny cannot be formally determined. Nevertheless, the widespread conservation of the second acidic residue across the MutL, GyrB, and MORC lineages, together with the high posterior probability at the most recent common ancestor of these groups and Hsp90, indicates that this residue was very likely to be present in their ancestor. Its absence within the Hsp90 lineage is therefore most parsimoniously interpreted as lineage-specific loss. In summary, these results suggest that the Hsp90 lineage underwent remodeling of its ATPase catalytic mechanism during its evolutionary divergence from other GHKL ATPase family members.

Conclusions

In this study, we re-examined the catalytic mechanism of GHKL ATPases using aqMutL and aqGyrB as model systems with mutational, biochemical, and crystallographic studies. Our results reveal that ATP hydrolysis in these enzymes is not governed by a single general base residue, as has been traditionally assumed, but instead relies on the coordinated action of two conserved acidic residues. Structural analyses indicate that Glu48 of aqGyrB plays a dominant role in aligning the nucleophilic water molecule in an optimal geometry for attack on the γ-phosphate of ATP. However, biochemical and structural evidence from single and double mutant forms indicates that both residues contribute to proton abstraction from the nucleophilic water. Thus, general base catalysis in GyrB and MutL appears to be achieved by redundant proton-accepting residues.

Extending this finding to human MutL homologs, we showed that mutations at the corresponding residues in PMS2 and MLH1—reported as variants of uncertain clinical significance—lead to substantial or complete loss of the ATPase activity. Given that even modest reductions in the MutL ATPase activity are known to severely compromise mismatch repair efficiency *in vivo*, our findings suggest that these variants might be functionally deleterious. Thus, the mechanistic insights obtained in this study provide a structural and biochemical basis for evaluating the pathogenic potential of clinically ambiguous variants in human MutL homologs.

Materials and Methods

Construction of expression plasmids

Expression plasmids encoding mutant forms of the aqMutL NTD (residues 1–315), the aqGyrB NTD (residues 1–397), the human PMS2 NTD (residues 1–365), and the human MLH1 NTD (residues 1–337) were generated by introducing point mutations into pET-11a/*aqMutL NTD* [47], pET-11a/*aqGyrB NTD* [11], pCold ProS2/*human PMS2 NTD* [35], and pET28-MLH1/*human MLH1 NTD* [11] plasmids using the PrimeSTAR site-directed mutagenesis protocol (Takara). Primer sequences used for mutagenesis are listed in Supplementary Table S1. DNA sequencing confirmed that no unintended mutations were introduced.

Expression and purification of proteins

The wildtype aqMutL NTD, aqGyrB NTD, ProS2-tagged human PMS2 NTD, and His-tagged human MLH1 NTD were overexpressed and purified as described previously [11,35,47]. The mutant forms were overexpressed and purified using the same procedures as for the respective wildtype proteins.

CD spectrometry

CD measurements were performed with a spectropolarimeter, model J-720W (Jasco). Measurements of CD spectra were carried out in a solution comprised of 20 mM Tris-HCl (pH 8.0) (eLANT) and 10 μM protein using a 0.1 cm cell at 25°C. The residue molar ellipticity [Θ] was defined as 100 $\Theta_{obs}/(lc)$, where Θ_{obs} is the observed ellipticity, l is the length of the light path in centimeters, and c is the residue molar concentration of the protein.

ATPase assay

ATPase activities of the aqMutL NTD, aqGyrB NTD, ProS2-tagged human PMS2 NTD, and His-tagged human MLH1 NTD were measured as described previously [35]. Reactions were carried out using 10 μM protein in a 20 μl reaction mixture containing 50 mM HEPES–KOH (pH 7.5) (eLANT), 100 mM NaCl, 5 mM $MgCl_2$, and various concentrations of ATP (Roche). For the aqMutL NTD and aqGyrB NTD, reactions were performed at 70°C for 60 min. For the NTDs of the human MutL homologs, reactions were performed at 37°C for 120 min. All experiments were conducted in triplicate. Kinetic parameters were determined by fitting the data to the standard Michaelis–Menten equation using IgorPro.

Equilibrium dialysis

Equilibrium dialysis experiments were performed as described previously [11]. Seventy-five microliters of buffer containing 50 mM Tris–HCl (pH 8.0), 100 mM NaCl, 5 mM $MgCl_2$, and 50 μM AMPPNP (Roche) were loaded into the buffer chamber of a DispoEquilibrium Dialyzer equipped with a 10 kDa molecular weight cut-off membrane (Harvard Bioscience, Inc.). An equal volume of the aqMutL NTD (0–320 μM) or aqGyrB NTD (0–400 μM) in the same buffer without AMPPNP was placed in the opposing sample chamber. The device was gently agitated at room temperature for 24 h to allow equilibration. The absorbance of the solution in the buffer chamber was measured at 260 nm. The concentration of unbound AMPPNP was calculated using a molar extinction coefficient (ε_{260} = 15,400 M^{-1} cm^{-1}).

Crystallization and structure determination

Protein crystallization was performed by the sitting-drop vapor diffusion method at 20°C. One microliter of the aqGyrB NTDs (14 mg/ml) containing 0.6 mM AMPPNP (Roche) and 1 mM $MgCl_2$ was mixed with an equal volume of the reservoir solution and equilibrated against 500 μl of reservoir solution. For the wildtype and D51A mutant forms of the aqGyrB NTD, crystals were obtained using a reservoir solution containing 0.2 M ammonium acetate, 0.1 M HEPES (pH 7.5), and 45% (v/v) 2-methyl-2,4-pentanediol. The E48A mutant form was crystallized in 0.05 M cadmium sulfate hydrate, 0.1 M HEPES (pH 7.5), and 20% (w/v) polyethylene glycol 3,350. The E48Q mutant form was crystallized under identical conditions consisting of 30% (w/v) polyethylene glycol 400, 100 mM HEPES–NaOH (pH 7.5), and 200 mM sodium chloride. The D51N mutant form was crystallized in 0.1 M sodium malonate (pH 7.0) and 12% (w/v) polyethylene glycol 3,350. Crystals of the wildtype and E48A mutant forms were soaked in the respective reservoir solutions supplemented with 30% (v/v) glycerol before being flash-cooled in liquid nitrogen. Crystal of the D51N mutant form was transferred to the reservoir solution containing 30% (w/v) polyethylene glycol 3,350 prior to flash-cooling in liquid nitrogen. Crystal of the D51A mutant form was directly flash-cooled in liquid nitrogen without additional cryoprotection.

X-ray diffraction data were collected at beamline BL45XU in SPring-8 (Hyogo, Japan) at a wavelength of 1.000 Å and a temperature of −173°C. Data were automatically collected and processed using the ZOO system [48], in which data processing was assisted by KAMO [49]. The linearity of the Wilson plot was confirmed over the resolution range employed. Phases were determined by molecular replacement using Phaser with a search model predicted by AlphaFold2 [50]. Model building and manual correction were performed using COOT [51], and structural refinement was carried out with PHENIX refine [52]. Data collection and refinement statistics are summarized in Table 2. All figures illustrating the protein structures were generated using PyMOL (Schrödinger).

Phylogenetic analysis and Ancestral state reconstruction

The ATPase domains of representative GHKL superfamily members (MutL, GyrB, MORC, and Hsp90) were aligned using amino acid sequences extracted based on domain boundaries defined by structural correspondence. The multiple sequence alignment was trimmed using trimAl [53] to remove ambiguously aligned regions. Maximum-likelihood phylogenetic inference was performed using IQ-TREE (v3.0.1) [54,55]. Ancestral state reconstruction was performed on the fixed maximum-likelihood topology using IQ-TREE under the empirical Bayesian framework implemented with the selected amino acid substitution model. The state of the amino acid residue at the alignment position corresponding to aqMutL Glu32 or aqGyrB Asp52 was examined. Maximum-likelihood phylogenies were visualized and annotated using the Interactive Tree of Life (iTOL) web server [56]. Trees were displayed in a rectangular layout without specification of an external outgroup. For visualization purposes, branch lengths were not scaled and were displayed with equal lengths.

Supplementary Materials

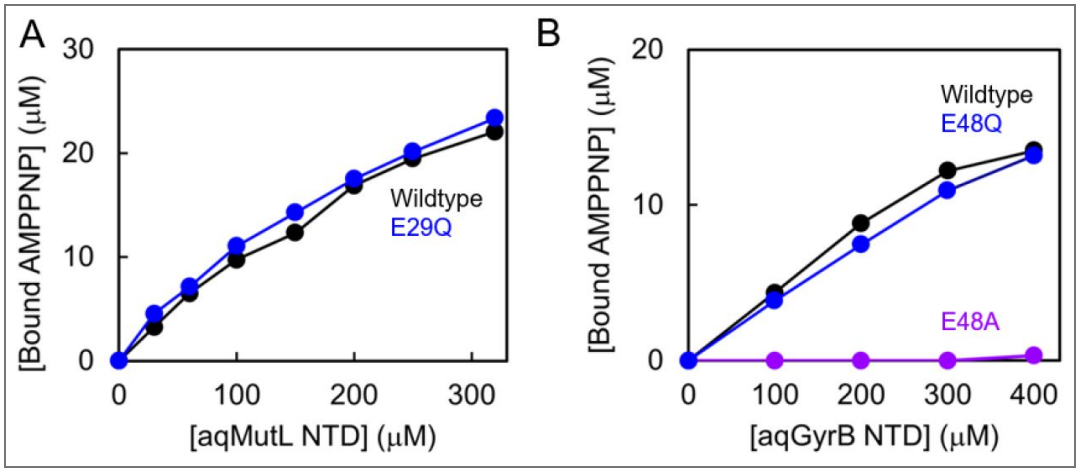

Supplementary Figure S1. The ATP-binding ability of the aqMutL NTDs (A) and aqGyrB NTDs (B). Binding affinities were quantified by equilibrium dialysis. For each protein concentration, the concentration of unbound AMPPNP was determined from the absorbance at 260 nm of the buffer chamber solution after equilibrium had been reached (see Materials and Methods). The concentration of bound AMPPNP was calculated by subtracting the concentration of unbound AMPPNP from the total AMPPNP concentration and was plotted against the protein concentration.

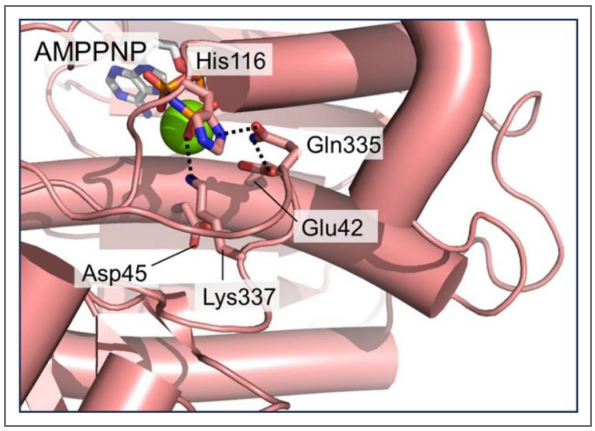

Supplementary Figure S2. Structure of the ATPase active site of the *E. coli* GyrB NTD.

Residues corresponding to Glu48, Asp51, His122, Gln340, and Lys342 of aqGyrB are Glu42, Asp45, His116, Gln335, and Lys337, respectively, in *E. coli* GyrB. Side chains of these residues are shown as stick models together with the bound AMPPNP. Hydrogen bonds and ionic interactions are depicted as dashed lines.

Target Protein	Mutation	Primer Name	Sequence (5′–3′)
aqMutL NTD	E32K	aqML_E32K_fw	ACTCGTTAAGAATTCTCTGGACGCAAA
		aqML_E32K_rv	GAATTCTTAACGAGTTCCTTTACGAC
	E32A	aqML_E32A_fw	CTCGTTGCGAATTCTCTGGACGCAAA
		aqML_E32A_rv	AGAATTCGCAACGAGTTCCTTTACGA
	E32V	aqML_E32V_fw	CTCGTTGTGAATTCTCTGGACGCAAA
		aqML_E32V_rv	AGAATTCACAACGAGTTCCTTTACGA
	E32G	aqML_E32G_fw	CTCGTTGGGAATTCTCTGGACGCAAA
		aqML_E32G_rv	AGAATTCCCAACGAGTTCCTTTACGA
	E32Q	aqML_E32Q_fw	CTCGTTCAGAATTCTCTGGACGCAAA
		aqML_E32Q_rv	AGAATTCTGAACGAGTTCCTTTACGA
	E29G	aqML_E29G_fw	GTAAAGGGACTCGTTGAGAATTCTCT
		aqML_E29G_rv	AACGAGTCCCTTTACGACGTCAACAG
	E29K	aqML_E29K_fw	GTAAAGAAACTCGTTGAGAATTCTCT
		aqML_E29K_rv	AACGAGTTTCTTTACGACGTCAACAG
	E29Q	aqML_E29Q_fw	CGTAAAGCAACTCGTTGAGAATTCTC
		aqML_E29Q_rv	ACGAGTTGCTTTACGACGTCAACAGG
	E29V	aqML_E29V_fw	GTAAAGGTACTCGTTGAGAATTCTCT
		aqML_E29V_rv	AACGAGTACCTTTACGACGTCAACAG
	E29Q/E32Q	aqML_E29Q/E32Q_fw	CGTAAAGCAACTCGTTCAGAATTCTC
		aqML_E29Q/E32Q_rv	ACGAGTTGCTTTACGACGTCAACAGG
aqGyrB NTD	D51A	aqGyrB_D51A_fw	ATACTTGCCAACGCCGTAGATGAGGC
		aqGyrB_D51A_rv	GGCGTTGGCAAGTATTTCCCAGATGA
	D51N	aqGyrB_D51N_fw	AATACTTAACAACGCCGTAGATGAGG
		aqGyrB_D51N_rv	GCGTTGTTAAGTATTTCCCAGATGAG
	E48A	aqGyrB_E48A_fw	ATCTGGGCAATACTTGACAACGCCGT
		aqGyrB_E48A_rv	AAGTATTGCCCAGATGAGGTGGTGAA
	E48Q	aqGyrB_E48Q_fw	ATCTGGCAAATACTTGACAACGCCGT
		aqGyrB_E48Q_rv	AAGTATTTGCCAGATGAGGTGGTGAA
	E48Q/D51N	aqGyrB_E48Q/D51N_fw	AATACTTAACAACGCCGTAGATGAGG
		aqGyrB_E48Q/D51N_rv	GCGTTGTtAAGTATTTGCCAGATGAG
human PMS2 NTD	E44Q	hPMS2_E44Q_fw	CCAGATGAAAGGCAAATTTTGCTAC
		hPMS2_E44Q_rv	TGCCTTTCATCTGGAGTAACATTGAT
	E44G	hPMS2_E44G_fw	TTAGTAGGAAACAGTCTGGATGCTGG
		hPMS2_E44G_rv	ACTGTTTCCTACTAACTCCTTTACCG
	E44V	hPMS2_E44V_fw	TTAGTAGTAAACAGTCTGGATGCTGG
		hPMS2_E44V_rv	ACTGTTTACTACTAACTCCTTTACCG
human MLH1 NTD	E37G	hMLH1_E37G_fw	ATGATTGGGAACTGTTTAGATGCAAA
		hMLH1_E37G_rv	ACAGTTCCCAATCATCTCTTTGATAG
	E37K	hMLH1_E37K_fw	GATGATTAAGAACTGTTTAGATGCAA
		hMLH1_E37K_rv	CAGTTCTTAATCATCTCTTTGATAGC
	E37Q	hMLH1_E37Q_fw	GATGATTCAGAACTGTTTAGATGCAA
		hMLH1_E37Q_rv	CAGTTCTGAATCATCTCTTTGATAGC

Supplementary Table S1. Primers used for site-directed mutagenesis in this study

Parameters	Wildtype	E48A	E48Q	D51A	D51N
Data collection					
Beamline	SPring-8 BL45XU	SPring-8 BL45XU	SPring-8 BL45XU	SPring-8 BL45XU	SPring-8 BL45XU
Detector	Dectris PILATUS 6M	Dectris PILATUS 6M	Dectris PILATUS 6M	Dectris PILATUS 6M	Dectris PILATUS 6M
Wavelength (Å)	1.0000	1.0000	1.0000	1.0000	1.0000
Exposure time (s)	0.02	0.02	0.02	0.02	0.02
Camera distance (mm)	140	140	140	140	140
Oscillation angle (∘)	0.1	0.1	0.1	0.1	0.1
Oscillation range (∘)	360	360	360	360	360
Space group	$P22_12_1$	$P6_422$	$P22_12_1$	$P22_12_1$	$P22_12_1$
Cell dimensions					

Supplementary Table 2. **Data collection and refinement statistics for the aqGyrB NTDs.**

a, *b*, *c* (Å)	78.9, 89.3, 126.3	173.1, 173.1, 80.1	74.5, 89.0, 131.3	75.2, 90.0, 131.7	70.0, 91.2, 131.1
α, β, γ (∘)	90.0, 90.0, 90.0	90.0, 90.0, 120.0	90.0, 90.0, 90.0	90.0, 90.0, 90.0	90.0, 90.0, 90.0
Resolution (Å)	43.16-1.65 (1.71-1.65) [a]	46.54-2.66 (2.76-2.66)	44.50-1.70 (1.76-1.70)	45.03-1.63 (1.70-1.63)	39.41-2.05 (2.12-2.05)
$I/\sigma I$	4.8 (1.3)	53.4 (15.8)	9.4 (1.3)	4.8 (1.4)	9.4 (1.4)
$CC_{1/2}$ (%)	99.0 (78.4)	99.2 (96.4)	99.7 (50.1)	96.4 (79.5)	99.5 (52.9)
R_{meas} (%)	2.3 (57.4)	20.9 (209.6)	18.4 (174.0)	22.8 (45.2)	20.7 (152.7)
Completeness (%)	99.3 (98.4)	100.0 (100.0)	99.9 (99.8)	99.6 (98.4)	99.9 (99.9)
Redundancy	8.1 (8.0)	14.2 (14.6)	7.1 (7.2)	4.1 (2.6)	7.0 (6.9)
Mosaicity (∘)	0.39	0.31	0.10	0.46	0.25
Refinement					
No. of reflections	107387	15381	96451	111409	53318
R_{work}/R_{free}	0.199/0.216	0.232/0.266	0.186/0.215	0.199/0.233	0.205/0.248
No. of atoms					
Protein	5660	2523	5766	5860	5758
Ligand/Ion	88	9	80	98	77
Water	285	7	588	227	379
B-factor					
Protein	34.1	77.4	25.0	35.5	29.5
Ligand/Ion	24.8	116.6	25.0	28.1	22.2
Water	34.6	64.1	33.4	34.4	30.6
r.m.s. deviations [b]					
Bond lengths (Å)	0.007	0.007	0.025	0.007	0.006
Bond angles (∘)	0.89	0.85	1.72	1.02	0.91
Ramachandran plot					
Most favored (%)	97.5	93.4	98.2	97.7	97.5
Additional allowed (%)	2.2	6.1	1.8	1.9	2.1
Generously allowed (%)	0.3	0.4	0	0.4	0.4
Disallowed (%)	0	0.1	0	0	0
Protein Data Bank Code	23UL	23UV	23UX	23UY	23UZ

[a]Values of the highest resolution shells.
[b]Root mean square deviations.

Supplementary Table 2. (continued)

Data availability

The structural data of WT, E48A, E48Q, D51A, and D51N mutant forms of the aqGyrB NTD are available at the protein data bank (*https://www2.rcsb.org/*) with accession numbers 23UL, 23UV, 23UX, and 23UZ, respectively.

Acknowledgements

The X-ray crystallographic experiments were performed at BL45XU in SPring-8, with the approval of JASRI (proposal nos. 2021A2758, 2021A2758, 2022A2729, and 2022B2729). The authors would like to thank the beamline scientists at SPring-8 BL45XU for their help in collecting the X-ray diffraction data.

Additional information

Author Contributions

KF and TY designed the research; KF, AS, and TM performed experiments; KF, AS, TM, and TY analyzed the data; KF and TY wrote the paper incorporating the opinions of all authors.

Funding

Funder	Grant reference number	Author
MEXT | Japan Society for the Promotion of Science (JSPS)	Grant-in-Aid for Scientific Research (C) (Basic Section 38030: Applied biochemistry), 24K08718	Kenji Fukui

Author ORCID iDs

Kenji Fukui: https://orcid.org/0000-0003-2463-7578

References

1 **Dutta R.,** Inouye M. (2000) GHKL, an emergent ATPase/kinase superfamily. *Trends in biochemical sciences* **25**:24-28 https://doi.org/10.1016/s0968-0004(99)01503-0 | PubMed

2 **Gellert M.,** Fisher L. M., O'Dea M. H. (1979) DNA gyrase: purification and catalytic properties of a fragment of gyrase B protein. *Proceedings of the National Academy of Sciences of the United States of America* **76**:6289-6293 https://doi.org/10.1073/pnas.76.12.6289 | PubMed

3 **Wigley D. B.,** Davies G. J., Dodson E. J., Maxwell A., Dodson G. (1991) Crystal structure of an N-terminal fragment of the DNA gyrase B protein. *Nature* **351**:624-629 https://doi.org/10.1038/351624a0 | PubMed

4 **Craig E. A.,** Gambill B. D., Nelson R. J. (1993) Heat shock proteins: molecular chaperones of protein biogenesis. *Microbiol Rev* **57**:402-414 https://doi.org/10.1128/mr.57.2.402-414.1993 | PubMed

5 **Marina A.,** Mott C., Auyzenberg A., Hendrickson W. A., Waldburger C. D. (2001) Structural and mutational analysis of the PhoQ histidine kinase catalytic domain. Insight into the reaction mechanism. *The Journal of biological chemistry* **276**:41182-41190 https://doi.org/10.1074/jbc.M106080200 | PubMed

6 **Glickman B. W.,** Radman M. (1980) Escherichia coli mutator mutants deficient in methylation-instructed DNA mismatch correction. *Proceedings of the National Academy of Sciences of the United States of America* **77**:1063-1067 https://doi.org/10.1073/pnas.77.2.1063 | PubMed

7 **Kadyrov F. A.,** Dzantiev L., Constantin N., Modrich P. (2006) Endonucleolytic function of MutLalpha in human mismatch repair. *Cell* **126**:297-308 https://doi.org/10.1016/j.cell.2006.05.039 | PubMed

8 **Pastor W. A.,** et al. (2014) MORC1 represses transposable elements in the mouse male germline. *Nat Commun* **5**:5795 https://doi.org/10.1038/ncomms6795 | PubMed

9 **Li S.,** et al. (2016) Mouse MORC3 is a GHKL ATPase that localizes to H3K4me3 marked chromatin. *Proceedings of the National Academy of Sciences of the United States of America* **113**:E5108-5116 https://doi.org/10.1073/pnas.1609709113 | PubMed

10 **Hu X.,** Machius M., Yang W. (2003) Monovalent cation dependence and preference of GHKL ATPases and kinases. *FEBS Lett* **544**:268-273 https://doi.org/10.1016/s0014-5793(03)00519-2

11 **Fukui K.,** Fujii Y., Yano T. (2024) Identification of a Catalytic Lysine Residue Conserved Among GHKL ATPases: MutL, GyrB, and MORC. *Journal of molecular biology* **436**:168575 https://doi.org/10.1016/j.jmb.2024.168575 | PubMed

12 **Piscitelli J. M.,** Manhart C. M. (2025) The GHKL ATPase Family as a Paradigm for MutL Homolog Function in DNA Mismatch Repair. *Int J Mol Sci* **26** https://doi.org/10.3390/ijms262412157 | PubMed

13 **Iyer L. M.,** Abhiman S., Aravind L. (2008) MutL homologs in restriction-modification systems and the origin of eukaryotic MORC ATPases. *Biol Direct* **3**:8 https://doi.org/10.1186/1745-6150-3-8 | PubMed

14 **Sacho E. J.,** Kadyrov F. A., Modrich P., Kunkel T. A., Erie D. A. (2008) Direct visualization of asymmetric adenine-nucleotide-induced conformational changes in MutL alpha. *Molecular cell* **29**:112-121 https://doi.org/10.1016/j.molcel.2007.10.030 | PubMed

15 **Maruya M.,** Sameshima M., Nemoto T., Yahara I. (1999) Monomer arrangement in HSP90 dimer as determined by decoration with N and C-terminal region specific antibodies. *Journal of molecular biology* **285**:903-907 https://doi.org/10.1006/jmbi.1998.2349 | PubMed

16 **Prodromou C.,** et al. (2000) The ATPase cycle of Hsp90 drives a molecular 'clamp' via transient dimerization of the N-terminal domains. *The EMBO journal* **19**:4383-4392 https://doi.org/10.1093/emboj/19.16.4383 | PubMed

17 **Fishel R.** (2015) Mismatch repair. *The Journal of biological chemistry* **290**:26395-26403 https://doi.org/10.1074/jbc.R115.660142 | PubMed

18 **Modrich P.** (2006) Mechanisms in eukaryotic mismatch repair. *The Journal of biological chemistry* **281**:30305-30309 https://doi.org/10.1074/jbc.r600022200 | PubMed

19 **Jiricny J.** (1998) Eukaryotic mismatch repair: an update. *Mutation research* **409**:107-121 https://doi.org/10.1016/s0921-8777(98)00056-1 | PubMed

20 **Putnam C. D.,** Kolodner R. D. (2023) Insights into DNA cleavage by MutL homologs from analysis of conserved motifs in eukaryotic Mlh1. *Bioessays* **45**:e2300031 https://doi.org/10.1002/bies.202300031 | PubMed

21 **Ban C.,** Junop M., Yang W. (1999) Transformation of MutL by ATP binding and hydrolysis: a switch in DNA mismatch repair. *Cell* **97**:85-97 https://doi.org/10.1016/s0092-8674(00)80717-5 | PubMed

22 **Rodriguez Gonzalez J.,** Davis C. L., Wilkins H., Erie D. A., Guarne A. (2025) Bacillus subtilis MutL samples multiple conformations during nucleotide binding and hydrolysis. *Structure* https://doi.org/10.1016/j.str.2025.12.007 | PubMed

23 **Shimada A.,** et al. (2013) MutS stimulates the endonuclease activity of MutL in an ATP-hydrolysis-dependent manner. *The FEBS journal* **280**:3467-3479 https://doi.org/10.1111/febs.12344 | PubMed

24 **Kadyrova L. Y.,** Kadyrov F. A. (2016) Endonuclease activities of MutLalpha and its homologs in DNA mismatch repair. *DNA repair* **38**:42-49 https://doi.org/10.1016/j.dnarep.2015.11.023 | PubMed

25 **Pillon M. C.,** et al. (2010) Structure of the endonuclease domain of MutL: unlicensed to cut. *Molecular cell* **39**:145-151 https://doi.org/10.1016/j.molcel.2010.06.027 | PubMed

26 **Jiricny J.,** Nystrom-Lahti M. (2000) Mismatch repair defects in cancer. *Current opinion in genetics & development* **10**:157-161 https://doi.org/10.1016/s0959-437x(00)00066-6 | PubMed

27 **Fishel R.,** Kolodner R. D. (1995) Identification of mismatch repair genes and their role in the development of cancer. *Current opinion in genetics & development* **5**:382-395 https://doi.org/10.1016/0959-437x(95)80055-7 | PubMed

28 **Fishel R.,** et al. (1993) The human mutator gene homolog MSH2 and its association with hereditary nonpolyposis colon cancer. *Cell* **75**:1027-1038 https://doi.org/10.1016/0092-8674(93)90546-3 | PubMed

29 **Lynch H. T.,** et al. (1985) Hereditary nonpolyposis colorectal cancer (Lynch syndromes I and II). I. Clinical description of resource. *Cancer* **56**:934-938 https://doi.org/10.1002/1097-0142(19850815)56:4<934::aid-cncr2820560439>3.0.co;2-i

30 **Kosinski J.,** Hinrichsen I., Bujnicki J. M., Friedhoff P., Plotz G. (2010) Identification of Lynch syndrome mutations in the MLH1-PMS2 interface that disturb dimerization and mismatch repair. *Human mutation* **31**:975-982 https://doi.org/10.1002/humu.21301 | PubMed

31 **Le D. T.,** et al. (2015) PD-1 Blockade in Tumors with Mismatch-Repair Deficiency. *N Engl J Med* **372**:2509-2520 https://doi.org/10.1056/NEJMoa1500596 | PubMed

32 **Mandal R.,** et al. (2019) Genetic diversity of tumors with mismatch repair deficiency influences anti-PD-1 immunotherapy response. *Science* **364**:485-491 https://doi.org/10.1126/science.aau0447 | PubMed

33 **Spampinato C.,** Modrich P. (2000) The MutL ATPase is required for mismatch repair. *The Journal of biological chemistry* **275**:9863-9869 https://doi.org/10.1074/jbc.275.13.9863 | PubMed

34 **Ban C.,** Yang W. (1998) Crystal structure and ATPase activity of MutL: implications for DNA repair and mutagenesis. *Cell* **95**:541-552 https://doi.org/10.1016/s0092-8674(00)81621-9 | PubMed

35 **Izuhara K.,** et al. (2020) A Lynch syndrome-associated mutation at a Bergerat ATP-binding fold destabilizes the structure of the DNA mismatch repair endonuclease MutL. *The Journal of biological chemistry* **295**:11643-11655 https://doi.org/10.1074/jbc.RA120.013576 | PubMed

36 **Drost M.,** et al. (2010) A cell-free assay for the functional analysis of variants of the mismatch repair protein MLH1. *Human mutation* **31**:247-253 https://doi.org/10.1002/humu.21180 | PubMed

37 **Aronshtam A.,** Marinus M. G. (1996) Dominant negative mutator mutations in the mutL gene of Escherichia coli. *Nucleic acids research* **24**:2498-2504 https://doi.org/10.1093/nar/24.13.2498 | PubMed

38 **Agrawal A.,** et al. (2013) Mycobacterium tuberculosis DNA gyrase ATPase domain structures suggest a dissociative mechanism that explains how ATP hydrolysis is coupled to domain motion. *The Biochemical journal* **456**:263-273 https://doi.org/10.1042/BJ20130538 | PubMed

39 **Brino L.,** et al. (2000) Dimerization of Escherichia coli DNA-gyrase B provides a structural mechanism for activating the ATPase catalytic center. *The Journal of biological chemistry* **275**:9468-9475 https://doi.org/10.1074/jbc.275.13.9468 | PubMed

40 **Feng L.,** et al. (2021) The pentapeptide-repeat protein, MfpA, interacts with mycobacterial DNA gyrase as a DNA T-segment mimic. *Proceedings of the National Academy of Sciences of the United States of America* **118** https://doi.org/10.1073/pnas.2016705118 | PubMed

41 **Fukui K.,** et al. (2017) Crystal structure and DNA-binding property of the ATPase domain of bacterial mismatch repair endonuclease MutL from Aquifex aeolicus. *Biochim Biophys Acta Proteins Proteom* **1865**:1178-1187 https://doi.org/10.1016/j.bbapap.2017.06.024 | PubMed

42 **Tan W.,** et al. (2025) MORC2 is a phosphorylation-dependent DNA compaction machine. *Nat Commun* **16**:5606 https://doi.org/10.1038/s41467-025-60751-z | PubMed

43 **Tencer A. H.,** et al. (2020) Molecular mechanism of the MORC4 ATPase activation. *Nat Commun* **11**:5466 https://doi.org/10.1038/s41467-020-19278-8 | PubMed

44 **Glaab W. E.,** et al. (1998) Resistance to 6-thioguanine in mismatch repair-deficient human cancer cell lines correlates with an increase in induced mutations at the HPRT locus. *Carcinogenesis* **19**:1931-1937 https://doi.org/10.1093/carcin/19.11.1931 | PubMed

45 **Bilwes A. M.,** Quezada C. M., Croal L. R., Crane B. R., Simon M. I. (2001) Nucleotide binding by the histidine kinase CheA. *Nat Struct Biol* **8**:353-360 https://doi.org/10.1038/86243 | PubMed

46 **Tanaka T.,** et al. (1998) NMR structure of the histidine kinase domain of the E. coli osmosensor EnvZ. *Nature* **396**:88-92 https://doi.org/10.1038/23968 | PubMed

47 **Iino H.,** et al. (2011) Characterization of C- and N-terminal domains of Aquifex aeolicus MutL endonuclease: N-terminal domain stimulates the endonuclease activity of C-terminal domain in a zinc-dependent manner. *Biosci Rep* **31**:309-322 https://doi.org/10.1042/BSR20100116 | PubMed

48 **Hirata K.,** et al. (2019) ZOO: an automatic data-collection system for high-throughput structure analysis in protein microcrystallography. *Acta Crystallogr D Struct Biol* **75**:138-150 https://doi.org/10.1107/S2059798318017795 | PubMed

49 **Yamashita K.,** Hirata K., Yamamoto M. (2018) KAMO: towards automated data processing for microcrystals. *Acta Crystallogr D Struct Biol* **74**:441-449 https://doi.org/10.1107/S2059798318004576 | PubMed

50 **Jumper J.,** et al. (2021) Highly accurate protein structure prediction with AlphaFold. *Nature* **596**:583-589 https://doi.org/10.1038/s41586-021-03819-2 | PubMed

51 **Emsley P.,** Lohkamp B., Scott W. G., Cowtan K. (2010) Features and development of Coot. *Acta Crystallogr D Biol Crystallogr* **66**:486-501 https://doi.org/10.1107/S0907444910007493 | PubMed

52 **Liebschner D.,** et al. (2019) Macromolecular structure determination using X-rays, neutrons and electrons: recent developments in Phenix. *Acta Crystallogr D Struct Biol* **75**:861-877 https://doi.org/10.1107/S2059798319011471 | PubMed

53 **Capella-Gutierrez S.,** Silla-Martinez J. M., Gabaldon T. (2009) trimAl: a tool for automated alignment trimming in large-scale phylogenetic analyses. *Bioinformatics* **25**:1972-1973 https://doi.org/10.1093/bioinformatics/btp348 | PubMed

54 **Nguyen L. T.,** Schmidt H. A., von Haeseler A., Minh B. Q. (2015) IQ-TREE: a fast and effective stochastic algorithm for estimating maximum-likelihood phylogenies. *Mol Biol Evol* **32**:268-274 https://doi.org/10.1093/molbev/msu300 | PubMed

55 **Minh B. Q.,** et al. (2020) IQ-TREE 2: New Models and Efficient Methods for Phylogenetic Inference in the Genomic Era. *Mol Biol Evol* **37**:1530-1534 https://doi.org/10.1093/molbev/msaa015 | PubMed

56 **Letunic I.,** Bork P. (2024) Interactive Tree of Life (iTOL) v6: recent updates to the phylogenetic tree display and annotation tool. *Nucleic acids research* **52**:W78-W82 https://doi.org/10.1093/nar/gkae268 | PubMed

57 **Thompson J. D.,** Higgins D. G., Gibson T. J. (1994) CLUSTAL W: improving the sensitivity of progressive multiple sequence alignment through sequence weighting, position-specific gap penalties and weight matrix choice. *Nucleic acids research* **22**:4673-4680 https://doi.org/10.1093/nar/22.22.4673 | PubMed

58 **Gouet P.,** Robert X., Courcelle E. (2003) ESPript/ENDscript: Extracting and rendering sequence and 3D information from atomic structures of proteins. *Nucleic acids research* **31**:3320-3323 https://doi.org/10.1093/nar/gkg556 | PubMed

Peer reviews

Reviewer #1 (Public review):

Summary:

In this manuscript, the authors study two residues in the GHKL ATPase active site of Aq MutL and GyrB, and argue that the catalytic base function is shared between two conserved acidic residues that are 3 residues apart.

They generated mutant versions in MutL and GyrB (both ala and the appropriate Asn/Gln version) and performed ATPase analysis. They also generated high-resolution crystal structures of the GyrB NTD with AMPPnP for WT and mutants of the two acidic residues. The data show that mutation in either of these residues does not fully kill activity (with the exception of the Alanine mutation of the first of the two, which interferes with ATP (or AMPPnP) binding). When the acidic residues are mutated to Asn/Gln, the catalytic water can

still be positioned, and hence these mutants are more active than the Ala mutants. In both cases, the double mutation is catalytically dead.

The authors then perform phylogenetic analysis and ancestral gene reconstruction, and based on this, they argue that HSP90 forms a different class of GHKL ATPases, and lost rather than gained this separate status.

Strengths:

The biochemical analysis seems solid.

Weaknesses:

(1) A major question that remains is why the mutations have so much more detrimental effect in MutL (100-fold lower kcat/KM) than they do in GyrB (3-fold lower). Can the authors explain this? Doesn't this argue against the proposed catalytic conservation?

(2) The structure figures all have omit maps for just the AMPPnP and the water, whereas the density for the acidic residues and their mutants is not shown.

https://doi.org/10.7554/eLife.111443.1.sa1

Reviewer #2 (Public review):

Summary:

In this manuscript, Fukui et al. re-examined the ATP hydrolysis mechanism in GHKL ATPases, revealing a cooperative role of two conserved acidic residues rather than one. The authors have used a range of biochemical and structural techniques on various mutants from different members of the GHKL ATPase family to test and validate their proposed mechanism.

Through a detailed re-analysis of their previously published structure of the aqMutL NTD (ATPase domain) in complex with AMPPCP, they identified Glu29 and Glu32 as interacting with nucleophilic water for the catalysis. The authors carefully dissected the respective roles of these two acidic residues with a series of site-directed mutations. Mutations at Glu29 impaired ATPase activity without affecting protein secondary structure or ATP binding in the case of the E29Q mutant. Moreover, mutations at Glu32 did not affect secondary structure (except for E32G) but reduced ATPase activity. Activity was abolished when both residues (E29Q/E32Q) were mutated.

The authors extended their study to another GHKL ATPase, aqGyrB. Their findings further supported the cooperative function of the corresponding acidic residues in aqGyrB (Glu48 and Asp51) during ATP hydrolysis. Mutation of these residues partially impaired ATP hydrolysis without affecting protein secondary structure. ATPase activity was completely lost in the double mutant E48Q/D51M. While the E48Q mutant retained the ability to bind ATP, the E48A mutant did not. High-resolution structures of the WT and E48A, E48Q, D51A, and D51N mutants of the aqGyrB NTD demonstrated that nucleophilic water positioning depended on these residues. E48 played a dominant role in water positioning and is critical for stabilising ATP lid formation and associated conformational changes, whereas D51 contributed cooperatively to catalysis.

The authors investigated the functional impact of mutating the corresponding residues in the human MutL homologs PMS2 and MLH1. Clinical variants consistently exhibited reduced or abolished ATPase activity, providing a potential molecular basis for Lynch syndrome through impaired DNA mismatch repair.

Lastly, through evolutionary analysis, the authors inferred that the second acidic residue was likely present in the common ancestor of MutL, GyrB, and MORC proteins, but was lost in the case of Hsp90.

Strengths:

(1) This study contains a detailed structural and biochemical analysis of a biologically important set of GHKL ATPases. The authors identify a second acidic residue that is conserved and contributes to catalysis in a large subset of GHKL ATPases. An updated and extended mechanistic model of ATP hydrolysis by this class of enzymes is proposed, which involves cooperative and partially overlapping roles for the catalytic residue pair. This revised mechanistic model is invaluable for the interpretation of clinical variants of GHKL ATPases such as PMS2 and MLH1.

(2) The work described was performed to an excellent and rigorous technical standard. The structural and biochemical data are sound. The evidence supporting the claims is compelling.

Weaknesses:

(1) The identification in this study of a second acidic residue contributing to catalysis but not absolutely essential for catalysis is a useful finding. However, given that many structures of GHLK ATPases have been determined with different nucleotide analogs bound and that the essential role of the first acidic residue is well established, the importance and scope of the advances described here remain focused within the field of study of GHKL ATPases.

(2) The authors assessed the consequences of variants in the human MutL homologs PMS2 and MLH1, but various other human GHKL ATPases contain clinically relevant variants, some of which have stronger disease associations than the mutations examined in this study. A broader analysis of the effect (or likely effect) of disease-linked mutations in GHKL ATPases would have strengthened this study.

(3) In MLH1, the E37K mutation completely abolishes ATPase activity, but the corresponding mutations in aqMutL, aqGyrB, and PMS2 do not. It remains unclear why E37K in MLH1 leads to complete loss of activity, as the authors propose that water molecule positioning via the first acidic residue, as well as ATP lid stabilisation and associated conformational changes, should still be possible.

(4) The authors do not examine ATP binding in the E32 mutants of aqMutL NTD and the D51 mutants of aqGyrB, or AMPPNP binding of the NLH1 and PMS2 mutants. Hence, the relative contributions of the acidic residues to ATP binding and hydrolysis remain partially unclear.

(5) The ATPase assays for PMS2 and MLH1 (Figure 7 and Table 1) were performed with purification/solubility tags still present. Hence, it cannot be ruled out that these tags influence the measured activities.

(6) The authors suggest that the two-acidic-residue mechanism proposed in this study could be shared among several GHKL ATPase families, yet they also state that the hydrogen-bonding network was not observed in MutL and MORC family proteins. This raises doubt about how conserved the mechanism is, e.g., in MutL and MORC proteins.

https://doi.org/10.7554/eLife.111443.1.sa0